

# CHEMICAL COMPOSITION AND MICROSTRUCTURE OF Ti(C, N)-TiN COATING<sup>①</sup>

Ma, Liuying

*Department of Materials Science and Engineering,  
Central South University of Technology, Changsha 410083, China*

Bian, Hengzhen Liu, Guochun  
*Zhuzhou Cemented Carbides Plant, Zhuzhou 412000, China*

## ABSTRACT

Texture characters of TiN crystal as well as chemical composition, constituent phases and their distribution along depth of hard alloy Ti(C, N)-TiN coating were studied by means of Ar<sup>+</sup> sputtering, XPS and XRD. The results showed that surface layer is rich in titanium, nitrogen, oxygen and carbon; that cobalt diffuses from substrate to surface; that surface layer and its vicinity are composed of TiN, TiO<sub>x</sub>, CoO and trace amount of TiC; and that there occur TiO<sub>x</sub> compounds which were determined by XRD analysis. The results also indicate that concentrations of carbon and oxygen decrease sharply while that of titanium increases sharply with increasing depth; that volume ratio of TiN/TiO<sub>x</sub> varies from 1.5:1 to 1:0 gradually; that oxidation rate of the cobalt being faster than its diffusion rate gives rise to cobalt-poor region; and that existence of metallic oxides, strong {200} TiN texture and surface pores, inhomogeneity of grain sizes and non-perfect densification have harmful effects on mechanical properties of the coating.

**Key words:** chemical composition Ti(C, N)-TiN coating microstructure XPS XRD

## 1 INTRODUCTION

Ti(C, N)-TiN films have the advantages of high microhardness and excellent wearability. There are many ways to coat TiN films, and the quality of the coatings is getting better and better<sup>[1-3]</sup>. The chemical compositions and microstructures of the hard alloy coatings have direct relationships with the coating processes and technological parameters<sup>[1, 2, 4]</sup>. The differences in composition distribution and microstructure in the coatings prepared by same process can give rise to great differences in their mechanical properties, e. g. microhardness up to 20%.

By means of XRD and XPS analyses, the constituent phases, preferred orientation, chemical composition distribution and chemical states were studied.

## 2 EXPERIMENTAL

After the hard alloy substrate having been polished and ultrasonic wave cleaned, a Ti(C, N)-TiN film of 3 μm thickness was coated by plasma chemical vapour deposition at 450~600 °C.

Using a light load Vicker's tester, the microhardness of the substrate and the coating were determined to be 1 475 kgf/mm<sup>2</sup>

① Manuscript received April 9, 1993

and 1 750 kgf/mm<sup>2</sup> respectively. After having been cleaned by acetone and ultrasonic wave, the coated samples underwent 1~80 min of sputtering in the Ar<sup>+</sup> cleaning apparatus fixed on a MICROLAB MK II type electronic energy spectrometer. The Ar<sup>+</sup> current is 20 μA. The coating was activated by AlK<sub>α</sub> radiation and the XPS were automatically collected. The changes of chemical compositions and relative amounts along the coating depth were analysed. The chemical states of the elements and their changes along depth were determined by analysing the displacements of the high resolution XPS peaks. The surface layer charging effect of the samples were corrected using the Ar<sub>2p3/2</sub> peak. The constituent phases and preferred orientation were researched by a D-500 type X-ray diffractometer.

### 3 RESULTS AND DISCUSSION

Fig. 1 shows the change of the XPS of the coating along depth. According to the following formula [5]:

$$C_x = \frac{I_x}{S'_x} / \sum_i \frac{I_i}{S'_i}$$

the photoelectronic intensities of main peaks were changed into atomic per cent (Fig. 2).

The bonding energies calculated using main peaks' intensities of the high resolution XPS are listed in Table 1. The high resolution XPS of Ti<sub>2p</sub> and N<sub>1s</sub> are shown in Fig. 3.

Figs. 1 and 2 indicate that after undergoing 1~10 min of Ar<sup>+</sup> sputtering, the amounts of oxygen and carbon are much larger than those of titanium and nitrogen. With increasing Ar<sup>+</sup> sputtering time, i. e. with increasing depth, the amounts of oxygen and carbon decrease sharply, and those of titanium and nitrogen increase sharply. After 50 min of Ar<sup>+</sup> sputtering, the

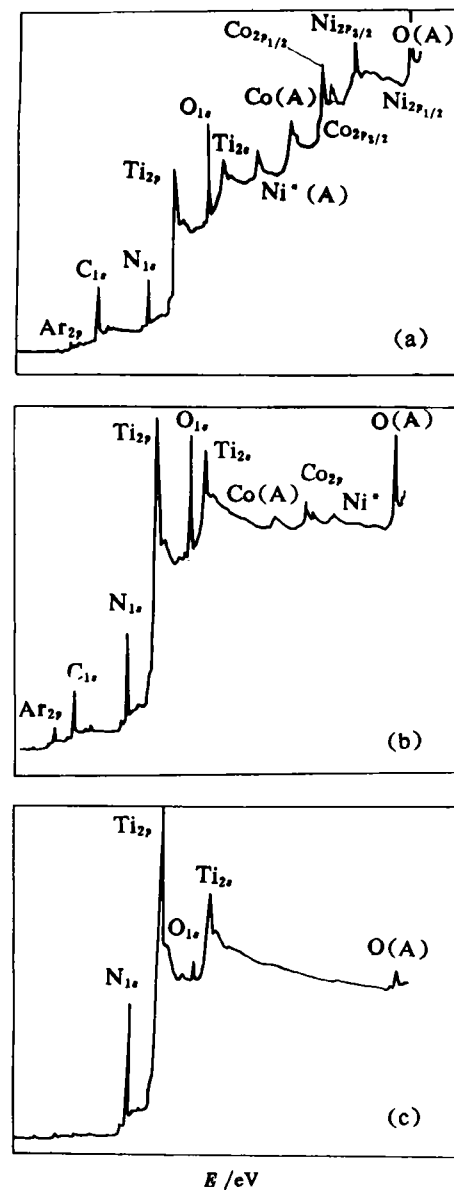


Fig. 1 XPS patterns of TiN coating

(a)—Ar<sup>+</sup> sputtering for 1 min,  
 (b)—Ar<sup>+</sup> sputtering for 20 min,  
 (c)—Ar<sup>+</sup> sputtering for 80 min;  
 (A)—Auger signal; \*—signal of sample holder

amounts of oxygen and carbon are stabilized at ~ 5 at.-%, and titanium at ~ 40 at.-%. When the sputtering time reached 80 min, the Ti/N ratio approximately equaled 0.85, which also means that the

Table 1 Chemical states and constituent phases in TiN coating determined by XPS analysis

Time of Ar <sup>+</sup> sputtering /min	Konding energies of valence electrons/eV				Constituent phases	TiN : TiO <sub>x</sub>
	Ti <sub>2p</sub> <sub>3/2</sub>	Co <sub>2p</sub> <sub>3/2</sub>	C <sub>1s</sub>	N <sub>1s</sub>		
1	455. 0	779. 1	286. 8	397. 0	TiN, TiO <sub>x</sub> , CoO	1. 5:1
	~457. 7	~285. 0	~287. 0	~284. 5	TiN, TiO <sub>x</sub> , CoO	2. 4:1
20	455. 0	779. 0	287. 0	397. 4	TiN, TiO <sub>x</sub> , CoO	2. 4:1
	~457. 9	~284. 5	~287. 0	397. 8	TiN, TiO <sub>x</sub>	~1:0
80	455. 1	/	287. 0	397. 8	TiN, TiO <sub>x</sub>	~1:0
	Standard bonding energy <sup>[5]</sup>	453. 8	778	287. 0	402	
	~454. 0					

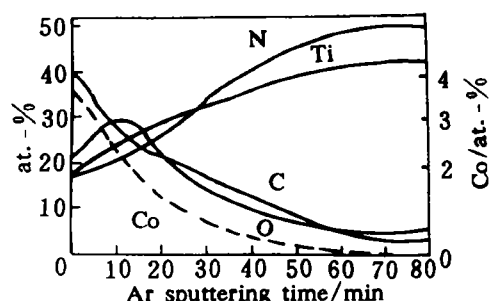


Fig. 2 Change of coating composition along depth

Ar<sup>+</sup> sputtering was limited in the TiN layer and did not penetrate the Ti(C, N) layer. The concentration of cobalt on the surface can be up to 3.5 at.-%. But with increasing depth, it decreases to zero sharply, i. e. there occurs a cobalt-poor region between the external surface layer and the substrate.

Specific chemical environment determines the bonding energies of the inner-shell electrons of an atom, then influences the photoelectronic peak position in the XPS. Fig. 3 is the high resolution XPS which illustrates the influence of the chemical environment on the bonding energies of the inner shell electrons of the titanium and nitrogen atoms in the coating.

The values of the main peaks determined from the high resolution XPS of Ti<sub>2p</sub>, Co<sub>2p</sub>, C<sub>1s</sub> and N<sub>1s</sub> of the coating are listed in

Table 1. The bonding energy of the 1s electrons of a neutral carbon atom is 287eV<sup>[5]</sup>. The C<sub>1s</sub> bonding energy data in Table 1 show that there are two C<sub>1s</sub> peaks in the surface layer, i. e. 286.8~287 eV, 285.0~284.5 eV. The former corresponds to the physical adsorption of the sample to carbon, the latter corresponds to TiC. The experimental C<sub>1s</sub> peaks show that the amount of bonded titanium is very small. Fig. 3 also indicates that the titanium almost does not occur in the form of TiC. Therefore, only in the surface layer, there occurs trace amount of TiC. After 80min of Ar<sup>+</sup> sputtering, only one peak of C<sub>1s</sub> is left over, and its bonding energy is 287 eV.

The bonding energy of 2p<sub>3/2</sub> electrons of metallic cobalt is 778 eV<sup>[5]</sup>. In the coating, the bonding energy of Co<sub>2p</sub><sub>3/2</sub> electrons is 779~779.1 eV (Table 1). It is evident that there occurs chemical displacement. The bonding energy of Co<sub>2p</sub><sub>3/2</sub> in CoO is 779.5~780.8 eV. This means that the cobalt in the coating occurs in the form of CoO and there is no metallic cobalt. Formation of cobalt-poor region between the coating exterior and the substrate can be attributed to that the oxidation rate of the cobalt is higher than its diffusion rate from the substrate to the surface.

The Ti<sub>2p</sub><sub>3/2</sub> peak splits into two peaks, and there occur chemical displacements in

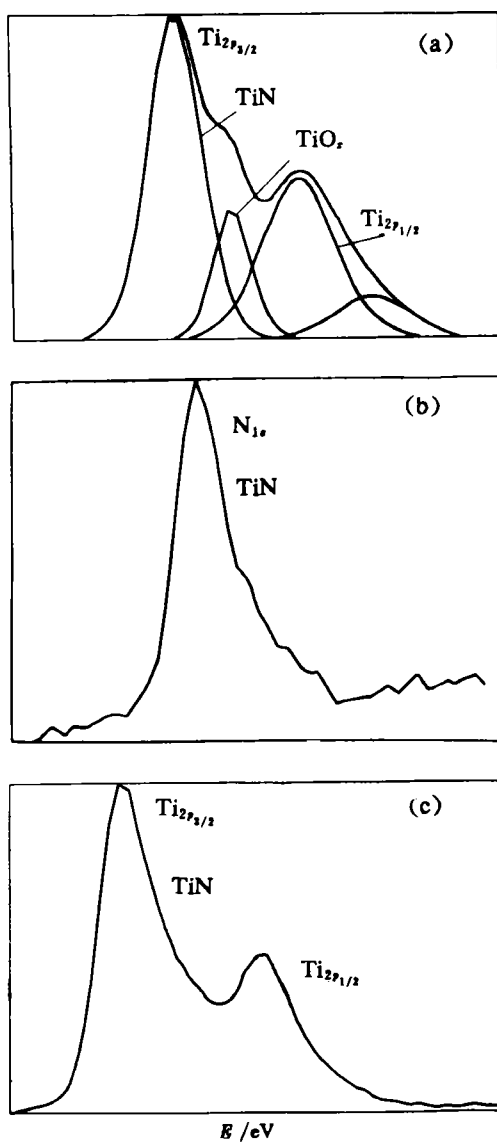


**Fig. 3 High resolution XPS of  $\text{Ti}_{2p}$  and  $\text{N}_{1s}$**   
 (a)— $\text{Ti}_{2p}$  peak,  $\text{Ar}^+$  sputtering for 20 min;  
 (b)— $\text{N}_{1s}$  peak,  $\text{Ar}^+$  sputtering for 80 min;  
 (c)— $\text{Ti}_{2p}$  peak,  $\text{Ar}^+$  sputtering for 80 min

these two peaks. Ref. [5] listed the bonding energies of  $\text{Ti}_{2p_{3/2}}$  electrons in  $\text{TiN}$ ,  $\text{TiO}_2$  and  $\text{TiO}$ , and the corresponding values are  $454.8 \sim 455$  eV,  $458.3 \sim 459$  eV and  $453.7$  eV. Comparing the bonding energies with our experimental data, we can conclude that the titanium occurs in the forms of

$\text{TiN}$  and  $\text{TiO}_x$  ( $1 < x < 2$ ) and no metallic titanium and  $\text{Ti}(\text{C, N})$  have been found.

Fig. 3 (c) is the  $\text{N}_{1s}$  photoelectronic peak. When the  $\text{Ar}^+$  sputtering time is within  $1 \sim 80$  min, the peak profile remains unchanged but there occurs a negative drift of  $4.2 \sim 5.0$  eV. This means that nitrogen mainly occurs in the form of  $\text{TiN}$ . Fig. 1 indicates  $\text{Ti}:\text{N} < 1$ , there seems to be uncombined neutral nitrogen. But in consideration of the selective sputtering effect of the  $\text{Ar}^+$  and introducing selective sputtering coefficients<sup>[4]</sup>, the ratio of  $\text{Ti}/\text{N}$  approaches 1 or is larger than 1.

It is evident from the high resolution XPS that with increasing depth, the titanium compounds change from  $\text{TiN} + \text{TiO}_x$  mixture to single  $\text{TiN}$ , and the ratio of  $\text{TiN}/\text{TiO}_x$  can be estimated using the area ratio of the two sub-peaks of the  $\text{Ti}_{2p_{3/2}}$  photoelectronic peak. The results are listed in Table 1. The data in Table 1 indicate that  $\text{TiN}$  is the main phase of the whole external coating. The XRD analysis results of the coating's microstructure are listed in Table 2. The XPS analysis proved that the oxygen and oxides are only concentrated on the surface and in the surface layer, but the total amount of  $\text{TiO}_x$  exceeds the sensitivity of XRD analysis. No emergence of  $\text{CoO}$  and  $\text{TiC}$  peaks in the XRD indicates that the amounts of  $\text{CoO}$  and  $\text{TiC}$  in the coating are very small.

**Table 2 XRD analysis results of coating**

Constituent phases	Relative intensities of main $\text{TiN}$ peaks	Corresponding values in PDF card	Preferred orientation in $\text{TiN}$
$\text{TiN}$ ,	$\{111\}:\{200\}:$	$\{111\}:\{200\}:$	strong $\{200\}$
$\text{Ti}(\text{C, N})$ ,	$\{220\}$	$\{220\}$	preferred
$\text{TiO}_x$	$=30:100:6$	$=75:100:55$	orientation

$\text{TiO}_x$  and  $\text{CoO}$  are ionic compounds, and  $\text{TiN}$  is metallic compound. The micro-

hardness of the former two is lower than that of the latter. Therefore formation of metallic oxides will have harmful effects on the microhardness of the coating.

Table 2 indicates that TiN crystal displays strong  $\{200\}$  preferred orientation, then it is clear that most of the TiN grains parallel with the surface with  $\{200\}$  crystal faces. This will further bring unfavourable effects to the improvement of the microhardness.

The micrograph has some influence on the microhardness. Fig. 4 is the secondary electron SEM micrograph of the coating surface after 10 min of  $\text{Ar}^+$  sputtering. The grains arrange in rows and have great difference in size. These factors lower the microhardness of the coating to some extent.



Fig. 4 Secondary electron SEM micrograph of coating surface ( $\text{Ar}^+$  sputtering for 10 min)

#### 4 CONCLUSIONS

(1) The  $\text{Ar}^+$  sputtering was limited in the TiN layer, and did not penetrate the Ti (C, N) layer.

(2) The TiN surface and its vicinity are rich in oxygen and carbon. With increasing depth, their concentrations decrease sharply and those of titanium and nitrogen increase sharply. Finally the ratios of the above elements reached the normal values.

(3) The cobalt in the substrate diffused to the surface layer through heat diffusion, and was combined with oxygen to form  $\text{CoO}$ . The oxidation rate of the cobalt is higher than its diffusion rate, so that there formed a cobalt-poor region.

(4) The titanium was combined with nitrogen and oxygen and formed TiN and  $\text{TiO}_2$ . There formed a trace amount of TiC on the surface of the coating.

(5) The formation of metallic oxides, and strong  $\{200\}$  preferred orientation, the inhomogeneity of grain sizes and the existence of pores bring about unfavourable effects to the micro-hardness of the coating, and they contribute mostly to the lower micro-hardness of the specimens used in this paper.

#### REFERENCES

- 1 Liu, Guochun *et al.* Cemented Carbides, 1991, 8(2):20-33.
- 2 Zhou, Jiankun *et al.* Acta Metallurgical Sinica, 1990, 26(2):130-134.
- 3 Rossnagel, S M; Cuomo, J J. MRS Bull, 1987, 16:40.
- 4 Kuznetsov, M V. Thin Solid Films, 1992, (215):1-6.
- 5 Handbook of X-ray Photoelectrons Spectroscopy. USA PERKIN- ELMER Physical Electrons Division, 1978.